Biophysical Properties of Gap Junction Channels Formed by Mouse Connexin40 in Induced Pairs of Transfected Human HeLa Cells

Feliksas F. Bukauskas,* Claudia Elfgang,‡ Klaus Willecke,‡ and Robert Weingart*
*Physiologisches Institut, Universität Bern, CH-3012 Bern, Switzerland; and ‡Institut für Genetik, Universität Bonn, 53117 Bonn, Germany

ABSTRACT A clone of human HeLa cells stably transfected with mouse connexin40 DNA was used to examine gap junctions. Two separate cells were brought into physical contact with each other (*"induced cell pair"*) to allow insertion of gap junction channels and, hence, formation of a gap junction. The intercellular current flow was measured with a dual voltage-clamp method. This approach enabled us to study the electrical properties of gap junction channels (cell pairs with a single channel) and gap junctions (cell pairs with many channels). We found that single channels exhibited multiple conductances, a main state (γ_j*(main state)*), several substates (γ_j*(substates)*), a residual state (γ_j*(residual state)*), and a closed state (γ_j*(closed state)*). The γ_j*(main state)* was 198 pS, and γ_j*(residual state)* was 36 pS (temperature, 36–37°C; pipette solution, potassium aspartate). Both properties were insensitive to transjunctional voltage, V_j. The transitions between the closed state and an open state (i.e., residual state, substate, or main state) were slow (15–45 ms); those between the residual state and a substate or the main state were fast (1–2 ms). Under steady-state conditions, the open channel probability, P_o, decreased in a sigmoidal manner from 1 to 0 (Boltzmann fit: $V_{j,o} = -44$ mV; $z = 6$). The temperature coefficient, Q_{10}, for γ_j*(main state)* and γ_j*(residual state)* was 1.2 and 1.3, respectively ($p < 0.001$; range 15–40°C). This difference suggests interactions between ions and channel structure in case of γ_j*(residual state)*. In cell pairs with many channels, the gap junction conductance at steady state, g_j, exhibited a bell-shaped dependency from V_j (Boltzmann fit, negative V_j, $V_{j,o} = -45$ mV, g_j*(min)* = 0.24; positive V_j, $V_{j,o} = 49$ mV, g_j*(min)* = 0.26; $z = 6$). We conclude that each channel is controlled by two types of gates, a fast one responsible for V_j gating and involving transitions between open states (i.e., residual state, substates, main state), and a slow one involving transitions between the closed state and an open state.

INTRODUCTION

Our knowledge of structural and functional properties of gap junction channels has expanded quickly over the last few years. To some extent, this development was promoted by the availability of cDNAs encoding various connexin proteins. Expression studies with cDNA carried out on injected *Xenopus* oocytes and transfected cell lines have shown that different types of connexins are responsible for the functional diversity seen in gap junctions (e.g., Bennett and Verselis, 1992).

Mammalian connexin40 (Cx40) has been identified using PCR amplification or screening of genomic libraries of dog, rat, and mouse (Beyer et al., 1992; Haefliger et al., 1992; Hennemann et al., 1992; Kanter et al., 1992). Northern blot analysis of total RNA revealed that Cx40 is most abundant in lung, but is readily detectable in other tissues such as heart, kidney, skin, blood vessels, uterus, and ovary (Beyer et al., 1992; Haefliger et al., 1992; Hennemann et al., 1992; Kanter et al., 1992). Cx40 has been identified immunohistochemically in vascular endothelium (Bastide et al., 1993; Bruzzone et al., 1993) and heart (Bastide et al., 1993; Kanter et al., 1992; De Mazière et al., 1993; Gourdie et al., 1993; Gros et al., 1994). Sequence comparison of nucleotides and amino acids suggests that mouse Cx40 is more closely related to mouse Cx43 (α-subgroup of connexins) than to mouse Cx32 (β-subgroup). Furthermore, Cx40 is considered to be the mammalian homolog of chick Cx42 (Beyer et al., 1992).

Some functional aspects of Cx40 gap junctions have already been examined. For example, pairing of *Xenopus* oocytes previously injected with Cx40 cRNA leads to operational gap junctions. Their conductance, g_j, declines partially in response to the transjunctional voltage, V_j, thus yielding a symmetrical bell-shaped relationship $g_j = f(V_j)$ under steady-state conditions (Hennemann et al., 1992; Bruzzone et al., 1993; Ebihara, 1993). Or, coupling-deficient HeLa cells or SK-Hep-1 cells show intercellular dye transfer after transfection with Cx40 cDNA (Hennemann et al., 1992; Traub et al., 1994). Also, experiments on pairs of Cx40-transfected HeLa cells using voltage ramps and dual whole-cell recording reveal single-channel conductances of 121 and 153 pS, respectively (Eckert, 1993; Traub et al., 1994). However, the physiological data on Cx40 gap junctions gathered so far are hampered by methodological constraints. For example, because of low input resistance, paired oocytes lack an access to single-channel events. Or, pairs of transfected cells contain gap junctions with many channels and, hence, are not readily suitable for single-channel analysis.

The aim of the present project has been to examine further the biophysical properties of Cx40 gap junctions and gap junction channels adopting an alternative approach. Experiments were performed on a clone of HeLa cells stably transfected with DNA coding for Cx40 (Hennemann et al., 1992; Traub et al., 1994; Elfgang et al., 1994). Electrical measurements were carried out on *"induced pairs"* of cells using the dual voltage-clamp method (Bukauskas and Weingart,

Received for publication 4 November 1994 and in final form 6 March 1995.
Address reprint requests to R. Weingart, Physiologisches Institut, Universität Bern, Bühlplatz 5, CH-3012 Bern, Switzerland. E-mail: weingart@pyl.unibe.ch.

0006-3495/95/06/2289/10 $2.00

1994). This approach enabled us to examine both macroscopic and microscopic currents in the same preparation. In addition, it allowed us to determine conductances and kinetics of single channels with no ambiguity (Bukauskas and Weingart, 1994).

MATERIALS AND METHODS

Cells and culture conditions

Experiments were performed on HeLa cells derived from a human cervix carcinoma (ATCC code CCC2). The methods used to isolate genomic mouse Cx40 and to transfect Cx40 cDNA into the HeLa cells have been described previously in detail (Hennemann et al., 1992; Traub et al., 1994; Elfgang et al., 1994). Parental cells and transfectants were grown in DMEM containing 10% FCS, 100 μg/ml streptomycin, and 100 units/ml penicillin (code 2212, Seromed, Fakola, Basel, Switzerland). The cells were passaged weekly and diluted 1:10. For the experiments, monolayers of cells (~4 × 10^5 cells/cm^2) were harvested and resuspended in DMEM containing 10% FCS (cell density 0.2–1 × 10^6 cells/ml). Thereafter, the cells were seeded at a density of ~10^4 cells/cm^2 onto sterile glass coverslips placed in multiwell culture dishes. Electrical measurements were performed 1–3 days after plating.

Solutions

Experiments were carried out in modified Krebs-Ringer solution (mM): NaCl 140, KCl 4, $CaCl_2$ 2, $MgCl_2$ 1, glucose 5, pyruvate 2, HEPES 5 (pH 7.4). Patch pipettes were filled with saline containing (mM): Potassium aspartate 120, NaCl 10, MgATP 3, $MgCl_2$ 1, $CaCl_2$ 1, EGTA 10 (pCa ~ 8), HEPES 5 (pH 7.2), filtered through 0.22-μm pores.

Electrical measurements

Glass coverslips with adherent cells were transferred to the experimental chamber and superfused with modified Krebs-Ringer solution at 36–37°C. The experimental chamber, consisting of a Perspex frame with a glued-on glass bottom, was mounted on the stage of an inverted microscope equipped with phase-contrast optics (Diaphot-TMD, Nikon, Nippon Kogaku, Tokyo, Japan). Patch pipettes were pulled from glass capillaries (code GC150TF-10; Clark Electromedical Instruments, Pangbourne, U.K.) with a horizontal puller (DMZ-Universal, Zeitz-Instrumente, Augsburg, Germany). When filled with solution, the pipettes had D.C. resistances of 3–5 MΩ (tip diameter ~1–2 μm).

Two types of experiments were performed. In one case, two single cells were selected, brought into contact with two patch pipettes connected to separate amplifiers, and pushed against each other to induce the formation of gap junctions (*"induced cell pairs"*; Bukauskas and Weingart, 1994). In the other case, the two pipettes were connected to both cells of a cell pair spontaneously formed in culture (*"preformed cell pairs"*). In both configurations, a dual voltage-clamp method in conjunction with tight-seal, whole cell recording was used to control the membrane potential of the two cells individually and to measure the associated currents through both pipettes separately (Weingart, 1986). Initially, the membrane potential of both cells (cell 1, cell 2) was clamped to the same voltage, usually approximately −50 mV ($V_1 = V_2$). Thereafter, the membrane potential of one of the cells was changed to establish a junctional potential, $V_j = V_2 - V_1$. In the case of two separate cells, the currents measured with pipette 1 and pipette 2 correspond to current flow through the membrane of cell 1 (I_1) and cell 2 (I_2), respectively. In the case of a cell pair, a coupling current I_j of identical amplitude but opposite polarity is superimposed on I_1 and I_2.

Voltage and current signals were recorded with an FM tape recorder (SE 3000, SE Lab, Feltham, England). For analysis, the current signals were filtered at 1 kHz (8-pole Bessel; -3 dB) and digitized at 5 kHz with a 12-bit A/D converter (IDA 12120; Indec Systems, Capitola, CA, U.S.A.). Data acquisition and analysis was done with the software C-Lab (Indec Systems). Results are presented as means ± 1 SEM.

RESULTS

Formation of gap junctions and gap junction channels

Coverslips with adherent cells were screened visually for two single cells in close proximity. Each cell was then brought into contact with a patch pipette to form a gigaohm seal. After disruption of the membrane patches, the whole-cell recording conditions were established. The membrane potentials of cell 1 (V_1) and cell 2 (V_2) were clamped to different levels to provoke a sustained voltage gradient between the cells. Thereafter, the cells were maneuvered against each other by gently moving the patch pipettes by means of the micromanipulators.

Fig. 1 *A* illustrates the genesis of a gap junction with time. Values of the gap junction conductance (g_j) were determined and plotted as a function of time. Initially, a maintained V_j of 55 mV was present between the cells, later on a V_j pulse of 200 ms was administered to cell 1 once every second. Physical contact between the cells was established at time t = 0. After a delay of about 35 min, the first gap junction channel became apparent. Its conductance approximated 200 pS.

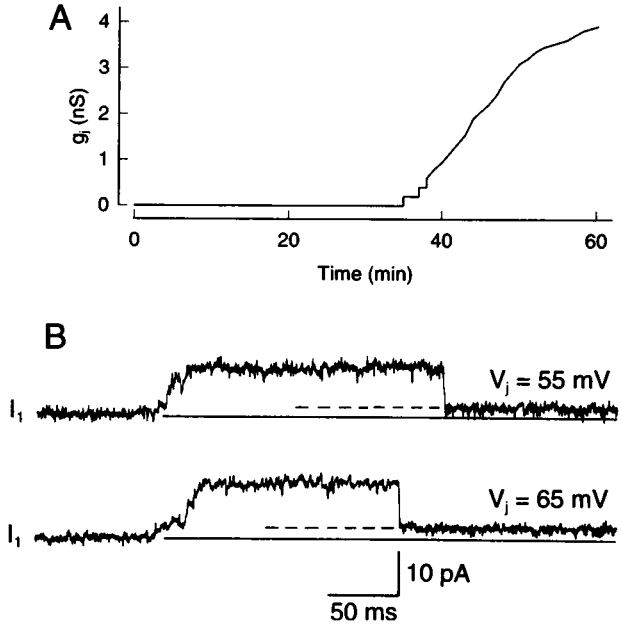

FIGURE 1 De novo formation of a gap junction between two single cells. (*A*) Plot of gap junction conductance, g_j, versus time. Time 0 indicates the moment of physical contact between the cells. The first sign of channel insertion was detectable 35 min later. Shortly after 60 min, the experiment came to an end because of the loss of a gigaohm seal. (*B*) Process of first channel insertion. Selected records of coupling current, I_1, associated with a transjunctional voltage gradient, V_j, of 55 mV (*top*) and 65 mV (*bottom*). Upward deflections correspond to channel openings. The first openings were slow and are associated with channel formation. Subsequent closings and openings were fast and are related to regular channel operation. The solid lines indicate the zero coupling current; the dashed lines indicate the residual current level.

Thereafter, g_j continued to increase in a saturating manner. The maximal rate of channel insertion was about 1 channel/min. At time t = 60 min, g_j approached a plateau corresponding to 20 channels. Utilizing the approach of *induced cell pairs*, we observed successful channel assembly in 7 out of 13 preparations. In these cases, the time to first channel insertion ranged from 26 to 45 min and the maximal g_j varied from 0.5 to 34 nS, depending on the duration of an experiment (average g_j = 13.0 ± 4.3 nS).

Fig. 1 *B* shows two examples of coupling current (I_j) documenting the event of a first channel opening. In these cases, V_j was set to 55 mV (upper trace) and 65 mV (lower trace). Starting from the zero current level (continuous line), I_j slowly increased to a plateau which corresponds to the fully open channel, I_j*(main state)*. The transition between the two levels was complete in 25 ms (upper trace) and 40 ms (lower trace) and was associated with irregular fluctuations. The analysis of I_j records obtained in this way yielded a value of 26 ± 7 ms (n = 6) for the duration of the slow transition associated with the first channel opening. After a variable time, I_j quickly decreased from I_j*(main state)* to a level which was distinctly different from zero and hence was named I_j*(residual state)* (interrupted line). This indicates that newly formed gap junction channels do not close completely under these conditions. The transition between I_j*(main state)* and I_j*(residual state)* was rapid, i.e. it elapsed within the response time of the experimental setup (transition time < 2 ms). This was also true for the subsequent channel operation (not shown). Examination of the current signals in Fig. 1 *B* revealed values for γ_j*(main state)* and γ_j*(residual state)* of about 190 pS and 38 pS, respectively.

Formation of a gap junction channel requires docking of two hemi-channels or connexons and subsequent channel opening. There was no change in holding current attributable to a leak before or during first opening of a gap junction channel. This implies that docking between two hemi-channels must be finished before a gap junction channel conducts.

Conductances of single gap junction channels

Fig. 2 *A* illustrates an experiment examining channel activity early during gap junction formation. A voltage pulse of 200 ms duration and -50 mV amplitude was administered to cell 2 once every second (V_2) while the membrane potential of cell 1 was maintained at -50 mV (V_1). The I_1 signals shown were gained from preparations whose gap junction consisted of one channel (upper trace) and two channels (lower trace). The I_j transitions evolving during the voltage pulse reflect gap junction channel events. In one case (upper trace), I_1 showed a fast transition between I_j*(main state)* and I_j*(residual state)* (dashed line). In the other case (lower trace), I_1 exhibited multiple transitions involving three discrete current levels emanating from 2 × I_j*(main state)*, I_j*(main state)* + I_j*(residual state)*, and 2 × I_j*(residual state)* (dashed line), respectively.

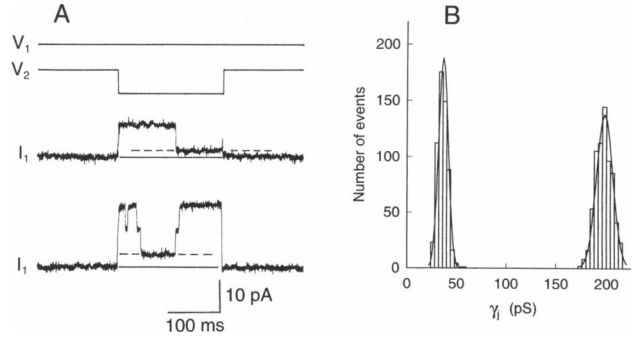

FIGURE 2 Gap junction channels exhibit a residual state and a main state. (*A*) Single-channel currents elicited by a transjunctional voltage gradient, V_j, of -50 mV (V_1 = -50 mV; V_2 = -100 mV). Coupling currents in the presence of one (*top I_1 trace*) and two (*bottom I_1 trace*) operational channels exhibit fast transitions between the residual state (- - - -) and main state. The solid lines indicate the zero coupling current. (*B*) Frequency histogram of single-channel conductances, γ_j. The left-hand distribution corresponds to γ_j*(residual state)* and revealed a mean value of 36.5 ± 0.4 pS (n = 569); the right-hand distribution corresponds to γ_j*(main state)* and yielded a mean value of 198.2 ± 0.6 pS (n = 687). Bin width = 4 pS.

To assess the single-channel conductances, we have analyzed current records obtained in the presence of maintained V_j gradients (see Fig. 1 *B*) or V_j pulses (see Fig. 2 *A*). In these experiments, the voltage gradient V_j was varied from 25 mV to 100 mV. Single channel conductances of the main state and residual state were determined as the ratio I_j*(main state)*/V_j and I_j*(residual state)*/V_j, respectively. There was no influence of V_j on conductance (γ_j*(main state)*: 2α > 0.1, slope = -0.016 pS/mV, r = 0.0134; γ_j*(residual state)*: 2α > 0.1, slope = -0.073 pS/mV, r = 0.257), hence all data were pooled for further analysis. The frequency histogram in Fig. 2 *B*, a plot of the number of events versus conductance, summarizes the results. The histogram shows two separate peaks which exhibit no overlap. The right hand peak revealed a mean value of 198.2 ± 0.6 pS (n = 687; range: 174 - 216 pS) and corresponds to γ_j*(main state)*; the left hand peak yielded a mean value of 36.5 ± 0.4 pS (n = 569; range: 25 - 58 pS) and corresponds to γ_j*(residual state)*. Hence, the ratio γ_j*(residual state)*/γ_j*(main state)* turns out to be 0.18.

Subconductance states

Associated with large V_j *gradients*, we often observed discrete current levels which were interposed between I_j*(main state)* and I_j*(residual state)*. This phenomenon is documented in Fig. 3. The records depicted originate from an induced cell pair whose gap junction consisted of a single operational channel. Repetitive application of a voltage pulse (200 ms, -75 mV) to cell 2 (V_2) provoked junctional currents with rapid flickering and involving levels different from I_j*(main state)* and I_j*(residual state)* (long dashes). As only one channel was present, all current transitions must have emerged from the same channel. Thus, we propose that the extra current levels (short dashes; top I_1 trace: 2 extra levels; middle and bottom I_1 trace: 1 extra level) reflect the existence of

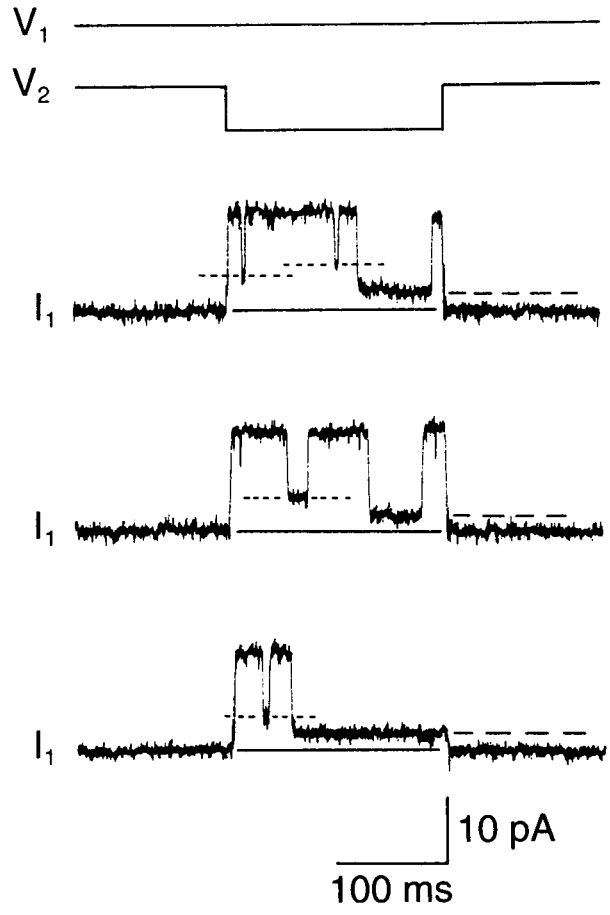

FIGURE 3 Evidence for multiple subconductances, γ_j*(substates)*. Voltage pulses were administered to cell 2 to establish a V_j of −75 mV (V_1 = −50 mV; V_2 = −125 mV) and to elicit coupling currents (I_1). In addition to the residual state (— — —) and the main state; the I_j signals revealed substates (- - - -). The records were obtained from an induced cell pair whose gap junction contained a single channel. γ_j*(substates)* = 64 and 90 pS (*top*), 70 pS (*middle*), and 64 (*bottom*).

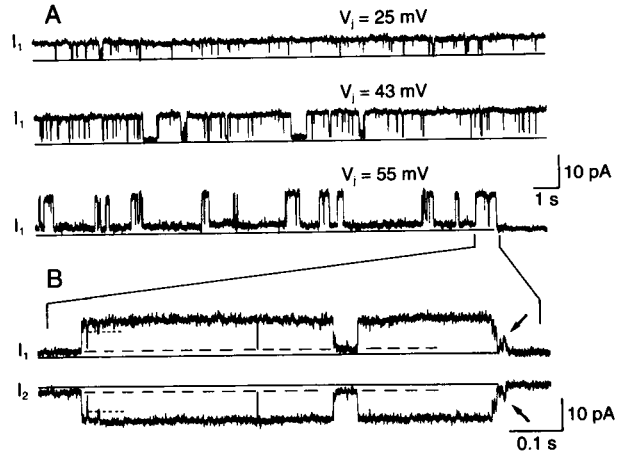

FIGURE 4 Effects of transjunctional voltage, V_j, on open channel probability, P_o*(main state)*. The preparation contained a gap junction with a single operational channel. (*A*) When V_j was increased from 25 mV (*top*) to 33 mV (*middle*) and 55 mV (*bottom*), the channel spent progressively less time in the fully open state, γ_j*(main state)* and more time in the residual state, γ_j*(residual state)*. Solid lines correspond to the fully closed state, γ_j*(closed)*. (*B*) Segments of I_1 and I_2 were recorded simultaneously and displayed at expanded time scale. V_j = 55 mV. Fast I_j transitions occur between γ_j*(main state)* and γ_j*(residual state)* (— — —) and between γ_j*(main state)* and a γ_j*(substate)* (- - - -). Slow I_j transitions occasionally occur between γ_j*(main state)* and γ_j*(closed)* (see *arrows*).

subconductance states, γ_j*(substate)*. Examination of the I_1 traces in Fig. 3 revealed a γ_j*(substate)* of 64 and 90 pS (top trace), 70 pS (middle trace) and 64 pS (bottom trace), respectively. From these data and others (see e.g. Fig. 4 *B*), we conclude that Cx40 channel possess several substates. Usually, the life time of the substates was considerably shorter than that of the residual state and/or the main state. Fast transitions between main state, substates, and residual state were typical for this mode of action (see Kinetic properties of single channels). Interestingly, substates were present preferentially early during the large V_j pulses. Similar results have been obtained from 5 additional preparations.

Open channel probabilities

Induced cell pairs which possess a single operational gap junction channel are ideal to examine channel kinetics. We found that under steady-state conditions, junctional currents preferentially flicker between two levels, I_j*(main state)* and I_j*(residual state)*. Hence, the analysis of such records allows an assessment of the open-state probability, P_o. The experimental protocol adopted for this study involved the application of V_j gradients of variable amplitude for prolonged periods of time (25 to 70 s). Fig. 4 *A* shows selected current records gained in this manner at V_j = 25 mV (top), 43 mV (middle), and 55 mV (bottom), respectively. A comparison of the I_1 signals suggests that the dwell time at discrete current levels is correlated with the amplitude of V_j. At 25 mV (top), the channel flickered rarely and was preferentially in the fully open state. At 43 mV (middle), the channel flickered more frequently and spent less time in the fully open state and more time in the residual state. At 55 mV (bottom), the channel exhibited fewer fast transitions again, but now spent most of the time in the residual state.

Long records like those depicted in Fig. 4 *A* were used to determine P_o. For analysis, the time spent in the main state was assessed and divided by the record duration. The values of P_o obtained in this way were plotted versus the amplitude of V_j. Fig. 5 shows the resulting plot. Each symbol corresponds to a single determination. The data points were fitted with the Boltzmann equation $P_o = \{(1 - P_o(min))/[1 + \exp(A(V_j - V_{j,o}))]\} + P_o(min)$; $P_o(min)$ is the minimal P_o at large V_j; $V_{j,o}$ corresponds to V_j at which P_o is half maximal; A is the maximal steepness of the relationship and expresses gating charge, $zq(kT)^{-1}$, where z is the equivalent number of unitary positive charges q moving through the entire electric field applied and k and T represent Boltzmann's constant and temperature in °K, respectively. The analysis yielded the following values: $V_{j,o}$ = 44.1 ± 1.5 mV, $P_o(min)$ = 0.06 ± 0.08; A = 0.23 ± 0.06; z = 6.0 ± 1.6.

Toward the end of the bottom record in Fig. 4 *A* (V_j = 55 mV), a rare phenomenon is apparent. The current changed

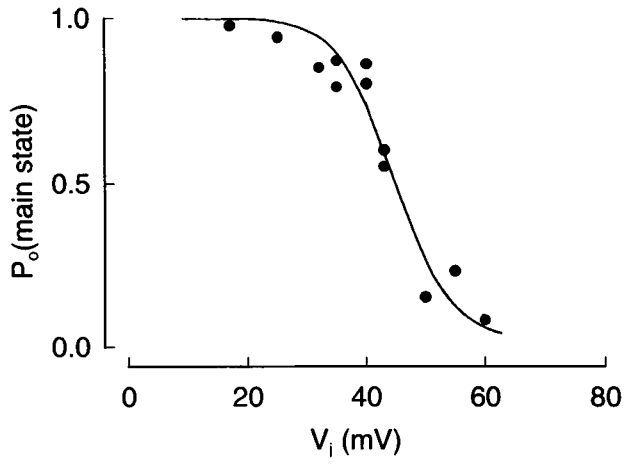

FIGURE 5 Dependency of open-state probability, $P_o(main\ state)$, on transjunctional voltage, V_j. Values of $P_o(main\ state)$ were determined from long current records (25–70 s) exhibiting single-channel activity (n = 12). (——) Best fit of data to the Boltzmann equation $P_o = \{(1 - P_o(min))/[1 + \exp(A(V_j - V_{j,o}))]\} + P_o(min)$; $P_o(min)$ = minimal P_o at large V_j; $V_{j,o}$ = V_j at which P_o is half maximal; A = maximal steepness of relationship; z: unitary positive charges moving through the electric field applied. Estimated parameters: $V_{j,o}$ = 44 mV, $P_o(min)$ = 0.06, A = 0.23, z = 6.

from $I_j(main\ state)$ to the reference level (*solid line*). This indicates that the channel is able to switch from the fully open state, $\gamma_j(main\ state)$, to a completely closed state, $\gamma_j(closed\ state)$. Fig. 4 *B* repeats the relevant I_1 sequence at expanded time scale. For clarity, it also includes the corresponding I_2. Close examination of these records reveals an additional property of gap junction channels: I_j undergoes two types of transitions, fast ones with transition times of <2 ms (frequency response of equipment), and slow ones with transition times of 12–45 ms (n = 18). As illustrated in Fig. 4 *B*, fast transitions were always observed between channel open states, i.e., the main state, the substates (see *pointed lines*), and the residual state. Hence, the residual state may be regarded as the resting state for fast channel operations. In contrast, slow transitions were seen between the closed state and any one open state, i.e., the main state, a substate, or the residual state (see *right-hand side*). Thus, the closed state may represent the resting state for slow channel operations. Typically, the slow transitions were irregular. Hence, they resemble the transitions associated with first channel openings (see Formation of gap junctions and gap junction channels). The current traces in Fig. 4 *B* also document the case of a $I_j(substate)$ with a short life time (see *arrow*), a rare event under steady-state conditions (see Subconductance states). In Fig. 4 *B*, each transition in I_1 has a mirrored counterpart in I_2. Corresponding transitions exhibit a similar amplitude and time course. Hence, they reflect gap junction channel events rather than artifacts.

Interactions between two symmetrical V_j-sensitive gates

It is generally agreed that a gap junction channel is composed of two hexameric hemi-channels or connexons and, thus, contains two symmetrical V_j-sensitive gates arranged in series. This raises the question whether I_j is controlled by the simultaneous operation of both gates. Fig. 6 illustrates the results of a set of experiments aimed at elucidating this question. Again, induced pairs whose gap junction consisted of a single channel were used. Fig. 6 *A* illustrates the pulse protocol adopted as well as a representative current trace. Initially, the membrane potential of both cells was clamped to the same level, i.e., $V_1 = V_2 = -50$ mV, hence, $V_j = 0$ mV. Thereafter, a biphasic voltage pulse was administered repetitively to cell 2 resulting in a V_j of −75 mV for 200 ms followed by a V_j of 50 mV for 100 ms. This protocol allowed the polarity of V_j to be reversed while changing its amplitude. As shown in Fig. 6 *A*, application of a negative V_j gradient led to a "net outward" I_1. At the beginning, the channel was in the main state, later on in the residual state (*dashed line*). Sudden application of a positive V_j gradient immediately provoked a "net inward" I_1 attributable to a residual state (*dashed line*). This suggests that the channel maintained its residual conductive state, irrespective of the polarity of V_j. After some delay (see *arrows*), the channel underwent a fast transition to its fully open state. This implies that inversion of the V_j polarity, after some delay, provoked the opening of a previously closed V_j-sensitive gate.

I_1 signals similar to that shown in Fig. 6 *A* were used to assess the delay for re-opening a closed V_j-gate. For this purpose, the time intervals between the incident of V_j polarity change and channel re-opening were determined. I_1 traces that exhibited a $I_j(residual\ state)$ for less than 50 ms before polarity reversal were rejected. The data obtained in this way from the same preparation were pooled in 5-ms time bins. Out of 512 trials, 49 revealed no re-opening during the positive V_j pulse (duration 100 ms) and, hence, were discarded. The remaining data were used to build the histogram illustrated in Fig. 6 *B*. It characterizes the kinetics of channel re-opening from the residual state. Obviously, the delay for re-opening was randomly distributed, i.e., short delays were

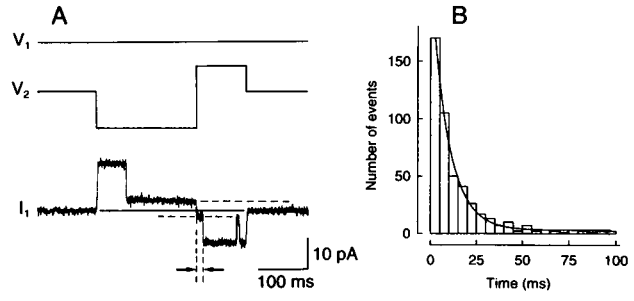

FIGURE 6 Restoration of single-channel activity. (*A*) Pulse protocol (V_1, V_2) and representative current record (I_1) documenting coupling currents. A biphasic voltage pulse was administered to cell 2 to establish a V_j gradient of −75 mV for 200 ms, followed by a V_j of 50 mV for 100 ms. Initially, V_1 and V_2 were set to −50 mV. Before V_j reversal, the channel was in the residual state (- - - -). Inversion of the V_j polarity led to a channel re-opening after a delay t = 12 ms (see *arrows*). (*B*) Frequency histogram of t, the time interval between the incident of V_j-polarity change and channel re-opening, determined in the same preparation (n = 463). (——) Best fit of data to a single exponential. Estimated time constant: τ = 9.5 ms.

much more frequent than long ones. The curve represents the best fit of the data to a single exponential revealing a time constant, τ, of 9.5 ms for a given voltage step.

Dependence of gap junction conductance on V_j

Intercellular current flow was also measured in cell pairs preformed in culture dishes. Out of 24 cell preparations examined, 19 were connected by gap junctions. The gap junctional conductance, g_j, was 21.4 ± 1.9 nS. The remaining five cell pairs were coupled by cytoplasmic bridges (see Bukauskas et al., 1992a, b). They revealed a junctional conductance of 25.6 ± 2.2 nS. To distinguish between gap junctions and cytoplasmic bridges, the preparations were routinely exposed to 100 μM arachidonic acid (AA). This fatty acid reversibly impairs current flow through gap junctions, but not through cytoplasmic bridges (Bukauskas et al., 1992a, b).

In five preformed cell pairs with gap junctions, the dependence of g_j on V_j was examined. To minimize problems arising from series resistances (see, e.g., Weingart, 1986; Bukauskas and Weingart, 1993a), measurements were made after washout of AA, i.e., during the recovery from uncoupling when g_j was low (<4 nS). The experimental protocol was as follows. At first, both cells were clamped to the same holding potential, $V_1 = V_2 = -50$ mV. Thereafter, voltage pulses of long duration (25–50 s), variable amplitude, and either polarity were applied to cell 1 to impose V_j gradients. Fig. 7 *A* shows selected records obtained from such an experiment. Depolarization of V_1 by 75 mV gave rise to an I_j undergoing a time-dependent decay (I_2, *left-hand side*). Hyperpolarization of V_1 by 75 mV led to a similar I_j of opposite polarity (I_2, *right-hand side*).

Fig. 7 *B* summarizes the results gained from the five preformed cell pairs and two induced cell pairs. The latter exhibited a g_j of 1.5 and 4 nS and, thus, exposure to AA was not required (see above). For analysis, the amplitude of I_j was determined at the beginning ($I_j(inst)$; inst = instantaneous) and end ($I_j(ss)$; ss = steady state) of each V_j pulse, and the ratios $g_j(inst) = I_j(inst)/V_j$ and $g_j(ss) = I_j(ss)/V_j$ were calculated. The values of $g_j(ss)$ were then normalized with respect to $g_j(inst)$ and plotted versus V_j. At large V_j, determinations of $I_j(inst)$ were inaccurate because of the frequency response of the equipment. Hence, under these conditions $g_j(inst)$ was determined from small test pulses (15 mV, 100 ms) administered repetitively to cell 1 between the long V_j pulses (see Fig. 7 *A*, *middle* part of V_1 and I_2). This procedure is applicable because $g_j(inst)$ is insensitive to V_j. The resulting graph yielded a bell-shaped relationship that was nearly symmetrical. The normalized $g_j(ss)$ was maximal over the V_j interval from approximately −25 to 25 mV. It decreased sharply at 25 mV < $|V_j|$ < 75 mV but did not drop to zero even at large V_j gradients. The smooth curve represents the best fit of the data to the Boltzmann equation, assuming that each channel contains two symmetrical gates in series: $g_j = \{(1 - g_j(min))/[1 + \exp(A(V_j - V_{j,o}))]\} + g_j(min)$; $g_j(min)$ is the normalized conductance at large V_j; $V_{j,o}$ corresponds to V_j at which g_j is half-maximal (see also Kinetic properties of

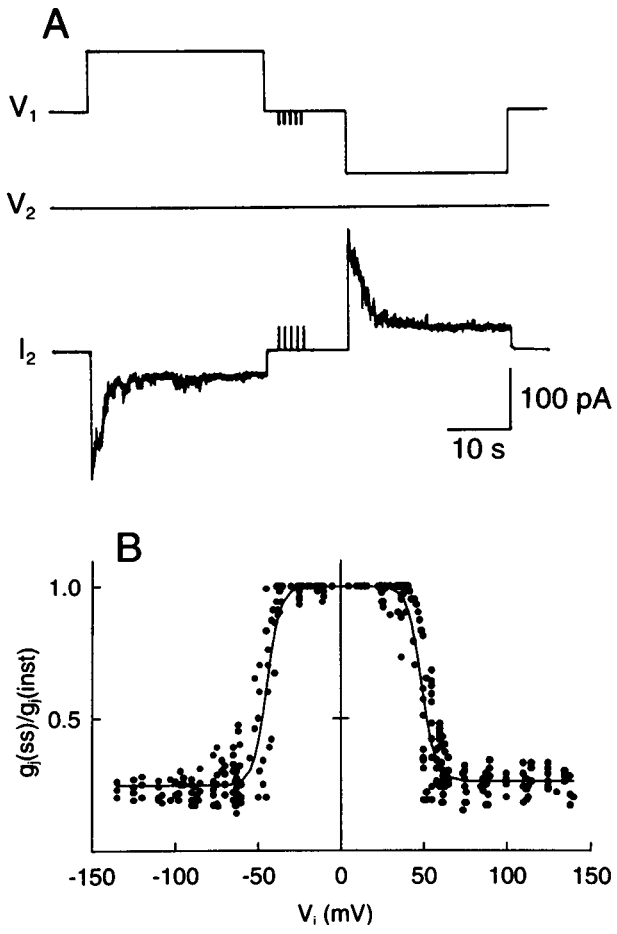

FIGURE 7 Dependency of gap junction conductance, g_j, on voltage gradient across the gap junction, V_j. (*A*) (V_1, V_2) Pulse protocol giving rise to a V_j of −75 mV (V_1 = 25 mV, V_2 = −50 mV: left-hand side) and 75 mV (V_1 = −125 mV, V_j = −50 mV; right-hand side). (I_2) Junctional currents exhibiting a time-dependent decay. (*B*) Relationship between g_j at steady state, $g_j(ss)$, and V_j. Each symbol corresponds to a single determination; number of preparations = 7. The smooth curve represents the fitted Boltzmann equation (see text) with $V_{j,o}$ = −44.9 mV (48.8 mV), $g_j(min)$ = 0.24 (0.26) for negative (positive) values of V_j, and z = 6.2 (5.9).

single channels). $V_{j,o}$ turned out to be −44.9 ± 0.6 and 48.8 ± 0.6 mV for negative and positive V_j gradients, respectively. The corresponding values of $g_j(min)$ were 0.24 ± 0.01 and 0.26 ± 0.01. *A*, which characterizes the steepness of $g_j(ss)/g_j(inst)$ changes, was 0.24 ± 0.03 and 0.23 ± 0.03 for negative and positive V_j gradients, respectively and, hence, z was 6.2 and 5.9 ($A = zq/(kT)^{-1}$).

Effect of temperature on single-channel conductance

In another series of experiments, we explored the effects of temperature on single-gap junction channels. Again, induced cell pairs with a single operational gap junction channel were used. The temperature of the bath solution was altered slowly. It was measured with a thermistor positioned close to the preparation, i.e., 0.5–1 mm (for details, see Bukauskas and Weingart, 1993a). The experimental protocol involved

repetitive application of V_j pulses (50 or 75 mV; 200 ms; 0.1 Hz) to one of the cells and determination of I_j(*main state*) and I_j(*residual state*). Fig. 8 summarizes the data obtained. Individual values of γ_j(*residual state*) (*bottom*) and γ_j(*main state*) (*top*) were calculated and plotted on a logarithmic scale versus temperature, T. Over the temperature range examined, i.e., 15–40°C, both I_j(*main state*) and I_j(*residual state*) decreased when the temperature was lowered. The solid lines were obtained by fitting the data to the exponential equation $\gamma_j = \gamma_{j,25} \times Q_{10}^{((T-25)/10)}$, where $\gamma_{j,25}$ is the conductance at $T = 25$°C, Q_{10} is the temperature coefficient, and T is the temperature (number of preparations = 3). The Q_{10} for γ_j(*main state*) and γ_j(*residual state*) was 1.21 ± 0.01 (number of measurements = 1650) and 1.30 ± 0.02 (number of measurements = 1445), respectively. Statistical analysis revealed that the values of Q_{10} are significantly difference from each other ($p < 0.001$), indicating that γ_j(*main state*) and γ_j(*residual state*) exhibit a different temperature sensitivity. This finding predicts that the ratio γ_j(*main state*)/γ_j(*residual state*) also exhibits a slight temperature dependence. Indeed, at $T = 15$, 25, and 40°C, this ratio was 0.163 (22 pS/135 pS), 0.175 (28.3 pS/162 pS), and 0.186 (38 pS/204 pS), respectively.

DISCUSSION

Previous studies on insect cells (Bukauskas and Weingart, 1994) have shown that induced cell pairs are suitable to study the de novo formation of gap junctions and gap junction channels and to examine the biophysical properties of these structures. Here we show that this experimental approach is also applicable to human HeLa cells transfected with mouse Cx40)

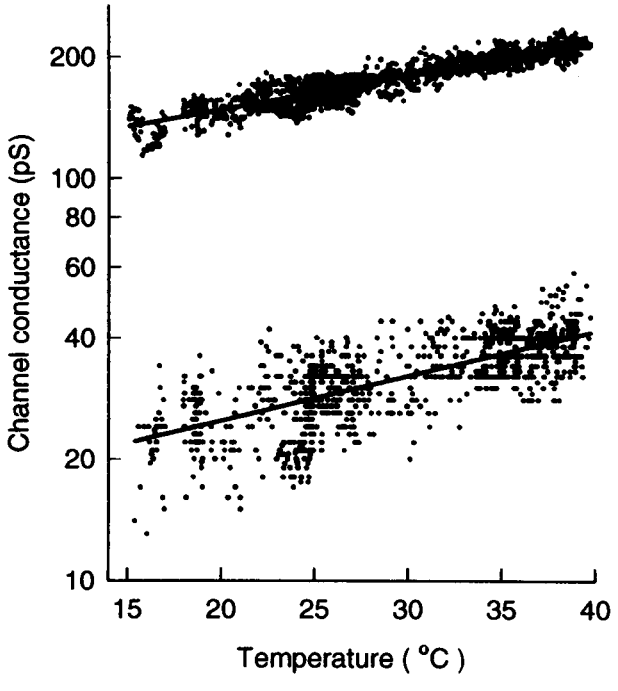

FIGURE 8 Influence of temperature, T, on single-channel conductances, γ_j. (*top*) Plot of γ_j(*main state*) versus T. (*bottom*) Plot of γ_j(*residual state*) vs. T. Each symbol corresponds to a single measurement (γ_j(*main state*): n = 1650; γ_j(*residual state*): n = 1445). Data were collected during application of V_j pulses of −50 or −75 mV amplitude. The temperature was changed continuously from 15–40°C. Solid lines represent fitted single-exponential equations (for details, see text). Q_{10} for γ_j(*main state*) and γ_j(*residual state*) was 1.2 and 1.3, respectively.

Formation of gap junction channels

It is generally agreed that formation of an operational gap junction channel involves docking of two hemi-channels or connexons. These channel precursors are thought to be present in the cell membrane as hexamers. Our data related to channel formation will be discussed within this framework.

Upon forcing two separate HeLa cells into physical contact, the first sign of a de novo formation of a gap junction channel was visible after 28–45 min (see Fig. 1 *A*). This delay is comparable with that found for neonatal rat heart cells (~30 min; Valiunas, Bukauskas, and Weingart, unpublished data), but considerably longer than that for insect cells, such as C6/36 cells (3–5 min; Bukauskas and Weingart, 1994) or hemocytes (2–35 s; Curchill et al., 1993). The difference between mammalian cells and arthropod cells may reflect a difference in 1) pool size of connexons in the plasma membrane, 2) lateral diffusion of connexons in the lipid bilayer, 3) connexon docking, or 4) cell-cell adhesion molecules in the plasma membrane (Musil et al., 1990).

Close inspection of the I_j signals provides some insight into the processes underlying formation of gap junction channels. For example, during channel formation there was no measurable current leak between the intra- and extracellular space. This indicates that the assembly of two connexons is complete *before* the gap junction channel starts to operate. Or, during the first channel opening, I_j always exhibited a slow transition (see Fig. 1 *B*), similar to that seen later on between γ_j(*main state*) and γ_j(*closed state*) on rare occasions (see Fig. 4 B; see also Fast and slow channel gating). This suggests that the slow gate of a gap junction channel is identical to the gate that keeps an isolated connexon closed. In fact, it has been proposed that before formation of gap junction channels, connexins are in a closed state, presumably because of a large $[Ca^{2+}]_o$ and the existence of a membrane potential (DeVries and Schwartz, 1992). Docking of two connexins may then trigger a channel-opening mechanism involving the slow gates. Furthermore, we also found that during the first channel opening, I_j slowly approached I_j(*main state*) before fast channel gating resumed (see Fig. 1 *B*). This indicates that in the isolated connexon the fast gate must be in the open state. In summary, our experiments on transfected HeLa cells support the idea that mammalian Cx40 gap junction channels, like insect gap junction channels (Bukauskas and Weingart, 1994), contain two types of gates, a fast one and a slow one (see Fast and slow channel gating).

Single-channel conductances

Using *induced cell pairs*, we were able to determine with no ambiguity the conductance of single-gap junction channels

of mammalian origin. After transfection with mouse Cx40, HeLa cells expressed gap junction channels exhibiting several conductance states, a fully open state (γ_j*(main state)*), a residual state (γ_j*(residual state)*), several substates (γ_j*(substate)*), and a closed state (γ_j*(closed state)*). Recently, a comparable study performed on an insect cell line, C6/36 (Bukauskas and Weingart, 1993b, 1994; Weingart and Bukauskas, 1993), neonatal rat heart cells, and transfected cells expressing Cx43 (Weingart, 1993) (Banach, Valiunas, Bukauskas, and Weingart, unpublished data), yielded similar results. This suggests that gap junction channels of different connexin composition operate in a similar manner.

γ_j*(main state)*

The mean value of γ_j*(main state)*, determined at 36–37°C, was 198 pS. Over the voltage range examined, γ_j*(main state)* was insensitive to V_j (25–100 mV). Eckert (1993) and Traub et al. (1994) examined the same transfectants in the *preformed cell pair* configuration at room temperature. They reported a single-channel conductance of 121 and 153 pS, respectively (pipette solution, 120 mM KCl). For comparison, in our study γ_j*(main state)* at 25°C was 162 pS (see Fig. 8). However, as shown previously (Bukauskas and Weingart, 1994), preformed cell pairs do *not* allow the identification of γ_j*(residual state)*. In this configuration, the analysis is likely to reveal *differences* between γ_j*(main state)* and γ_j*(residual state)*, but not γ_j*(main state)*.

γ_j*(residual state)*

In the presence of maintained V_j gradients (see Figs. 1 *A* and 4) or V_j pulses (see Figs. 2 *A*, 3, and 6), I_j usually flickered between two discrete levels corresponding to γ_j*(main state)* and γ_j*(residual state)*. This suggests that the channels failed to close completely under these conditions. The analysis revealed a mean γ_j*(residual state)* of 36 pS, a value 5.5 times smaller than γ_j*(main state)*. For comparison, in C6/36 insect cells the ratio γ_j*(main state)*/γ_j*(residual state)* was 5.8 (Bukauskas and Weingart, 1994). Experiments with preformed pairs of Cx40-transfected HeLa cells have shown that g_j does not decline to zero in the presence of a large V_j (see Fig. 7). This phenomenon has been observed in most types of gap junctions (for an exception, see Chanson et al., 1993). It can be explained readily by the existence of γ_j*(residual state)*. We propose that incomplete decline in g_j reflects partial channel closure rather than partial decline in open channel probability, P_o. With respect to the functional significance of γ_j*(residual state)*, we can only speculate at the moment. Conceivably, the transition from γ_j*(main state)* to γ_j*(residual state)* alters the selectivity of the channel. A general molecular coupling may turn into a selective molecular coupling or even give way to an ionic coupling. In this way, γ_j*(residual state)* could provide the basis for a mechanism of differential permeation. However, combined electrical and diffusional studies will have to provide the answer.

γ_j*(substates)*

When V_j was made larger than 50 mV, we observed additional discrete current levels. Because they were interposed between γ_j*(main state)* and γ_j*(residual state)*, they were called substates, γ_j*(substates)*. The current jumps between individual substates were variable. They revealed conductance steps ranging from 64 to 90 pS. Compared with γ_j*(residual state)*, the γ_j*(substates)* exhibited rather short life times, i.e., 2–30 ms (see Fig. 3). Substates were preferentially seen early during the application of V_j gradients of intermediate amplitude. This renders a quantitative study rather difficult. However, it raises interesting questions related to the operation of gap junction channels. The existence of substates suggests that V_j-sensitive gating involves subgates. Considering the hexagonal structure of a connexon, one is inclined to postulate that each V_j-sensitive gate consists of six subgates, i.e., each connexin, among other properties, serves the functional role of a subgate (see Bukauskas and Weingart, 1994). The preference of the channels for the transitions between γ_j*(main state)* and γ_j*(residual state)* indicates a high degree of cooperativity between the subgates.

Examining preformed pairs of vertebrate cells, several investigators have postulated substates for gap junction channels (see, e.g., Chen and DeHaan, 1992; Moreno et al., 1994). However, this approach renders it difficult to distinguish unambiguously among substates, several types of channels, and cooperativity between channels. Recently, Veenstra et al. (1994) described substates for Cx37 gap junction channels. To identify these events, junctional currents were recorded from preformed cell pairs and fitted with a probability density function.

Fast and slow channel gating

We found that I_j signals exhibit two types of transitions, fast ones that lasted 1–2 ms and slow ones that lasted 15–45 ms (see Figs. 1 *B* and 4 *B*). Fast transitions were abundant. They were associated with jumps between I_j*(main state)*, I_j*(substates)*, and I_j*(residual state)*, but never involved I_j*(closed)*. Slow transitions were rare. They were seen during the first opening of a newly formed channel (see Fig. 1 *B*). After formation of a channel, slow transitions between γ_j*(residual state)* and γ_j*(closed state)* were also observed occasionally. Interestingly, fast transitions stopped completely when a channel was in the closed state. It appeared that the incidence of slow transitions is not correlated with V_j. Our data are compatible with the following concept. Each channel possesses two types of gates, a fast one and a slow one. The fast gate is responsible for V_j-sensitive gating, and γ_j*(residual state)* may be regarded as its operational baseline. The slow gate keeps a hemi-channel in the closed state. It opens slowly during channel formation and is able to close the channel completely. Fast and slow transitions with such properties have also been observed in insect cells, i.e., C3/36 (Weingart and Bukauskas, 1993; Bukauskas and Weingart, 1994) and Sf9 (Bukauskas and Weingart, unpublished data).

As indicated in Fig. 1 *A*, induced cell pairs pass through a phase with only *one* operational gap junction channel present. This offers the opportunity to study channel kinetics under ideal conditions. We found that the probability of a channel to be in the main state, P_o, decreases with increasing V_j (see Fig. 4). The analysis revealed an inverse S-shaped relationship $P_o = f(V_j)$ with a $V_{j,o}$ of 44 mV and a gating charge $z = 6$ (see Fig. 5). This result is compatible with the view that each hemi-channel consists of 6 V_j-sensitive subgates that operate synchronously under these conditions.

Dependence of g_j on V_j

Under steady-state conditions, the HeLa transfectants exhibited a bell-shaped g_j/V_j relationship that was nearly symmetrical (see Fig. 7 *B*). Adopting the Boltzmann formalism, the analysis yielded the following parameters: $z = 6$; negative V_j: $V_{j,o} = -45$ mV, $g_j(min) = 0.24$; positive V_j: $V_{j,o} = 49$ mV, $g_j(min) = 0.26$. Together with the single-channel data, these results allow several conclusions. 1) The symmetry of the g_j/V_j relationship is compatible with the notion that a gap junction channel consists of two connexons, each containing a V_j-sensitive gate. However, it remains to be shown which V_j-polarity provokes closure of the gate (see, e.g., Suchyna et al., 1993). 2) Microscopic (see Kinetic properties of single channels) and macroscopic measurements led to the same value of V_j-gating charge, $z = 6$. Hence, both support the view that a connexon consists of six subunits or connexins, each possessing a V_j-sensitive subgate (Bukauskas and Weingart, 1994). 3) P_o declined to zero at large V_j (see Fig. 5). Therefore, $g_j(min)$ cannot be explained by a partial decrease of P_o. Instead, it is determined by the number of operational channels, n, and $\gamma_j(residual\ state)$. 4) Because $g_j(max)$ and $g_j(min)$ are dependent on $\gamma_j(main\ state)$ and $\gamma_j(residual\ state)$, $g_j(max)/g_j(min)$ should be equal to $\gamma_j(main\ state)/\gamma_j(residual\ state)$. However, the ratios turned out to be 4 and 5.8, respectively (see Single-channel conductances). Presumably, this discrepancy reflects an underestimate of $g_j(max)$ due to series resistance problems (Weingart, 1986). Hence, it documents the limitations of the accuracy of z and $V_{j,o}$ determinations. In essence, the parameters extracted from our macroscopic measurements are comparable with those reported previously for Cx40 expressed in preformed pairs of HeLa cells ($z = 4$, $V_{j,o} = 44$ mV; Eckert, 1993; Traub et al., 1994) and *Xenopus* oocytes (Hennemann et al. 1992): $z = 8$, $V_{j,o} = 35$ mV, $g_j(min) = 0.19$; Bruzzone et al. (1993): $V_{j,o} = 38$ mV, $g_j(min) = 0.18$; Ebihara (1993): $z = 4.3$, $V_{j,o} = 28$ mV, $g_j(min) = 0.3$).

Further insight into channel operation during V_j-gating was gained from the experiments examining the mechanism of channel re-opening (see Fig. 6). The I_j signals associated with an inversion of the V_j polarity suggest the following sequence of events. After a random length of time, t, the change in V_j polarity provokes re-opening of a V_j gate that was closed before. This then allows closure of a V_j gate of the same channel that was open previously. This leads to two conclusions: 1) each channel possesses two V_j-sensitive gates arranged in series; or 2) only one of the two gates is operational at any given time. The analysis of t revealed that restoration of the V_j gates follows an exponential time course. Within one time constant after inversion of V_j polarity, i.e., $\tau = 9.5$ ms, 63% of the channels underwent a transition from the residual state to the fully open state. This indicates that the recovery of the V_j gates is fast and is governed by a random process.

Temperature dependence of single-channel conductance

The motivation for this study was twofold: 1) to gain new insight into the biophysical properties of gap junctions and gap junction channels, and 2) to compare gap junction data gained at different temperatures. So far, most studies were carried out at room temperature.

We were interested to know whether $\gamma_j(main\ state)$ and $\gamma_j(residual\ state)$ exhibit the same temperature coefficient, Q_{10}. Varying the temperature from 15 to 40°C (see Fig. 8), the Q_{10} turned out to be 1.2 and 1.3 for $\gamma_j(main\ state)$ and $\gamma_j(residual\ state)$, respectively (see Fig. 8). The difference between these values was statistically significant ($p < 0.001$). For comparison, the Q_{10} for aqueous KCl solution is 1.2–1.3 (Robinson and Stokes, 1970). This implies that in case of the residual state, the permeation of small ions is slightly impaired by steric and/or electrical forces, whereas in case of the fully open state, it is not. For comparison, in neonatal rat heart cells we found a Q_{10} of 1.4 for the single-channel conductance (Bukauskas and Weingart, 1993a).

Intrinsic connexins

Parental HeLa cells contain an intrinsic connexin whose molecular structure has not been identified so far. We are confident that this connexin does not interfere critically with our Cx40 data for the following reasons. 1) The intrinsic connexin is expressed at a low level. For example, in preformed pairs of parental HeLa cells, g_j is 100 times smaller than in Cx40 transfectants (Eckert, 1993; Traub et al., 1994). 2) In parental HeLa cells, $\gamma_j(main\ state)$ is substantially smaller than in Cx40 transfectants (Eckert et al., 1993) (this paper). This difference offers an opportunity to distinguish between the two types of channels. However, in examining Cx40 transfectants with the induced cell pair approach, we never detected signs of intrinsic channels.

SUMMARY

Based on the data presented, we propose that Cx40-gap junction channels exhibit *two* gating mechanisms, a fast one controlled by V_j and a slow one whose control principle(s) remains obscure. The fast gating mechanism consists of six subgates. Their operation leads to fast current transitions among $\gamma_j(main\ state)$, $\gamma_j(substates)$, and $\gamma_j(residual\ state)$, but never involves $\gamma_j(closed)$. The slow gating mechanism

gives raise to slow current transitions. Slow transitions always start or end at γ_j*(closed)*, i.e., they occur between γ_j*(closed)* and any one open state. The coexistence of two types of gating mechanisms offers a variety of possibilities for the regulation of intercellular communication. Conceivably, γ_j*(residual state)* may serve to to discriminate between permeating molecules.

The authors acknowledge the expert technical assistance of Marlis Herrenschwand. We also thank Dr. Silvio Weidmann for valuable comments on the manuscript.

This work was supported by grants from the Swiss National Science Foundation (31–36'046.92) to R.W., the Deutsche Forschungsgemeinschaft (SFB 284, project C1), and the Fonds der Chemischen Industrie to K.W.

REFERENCES

Bastide, B., L. Neyses, D. Ganten, M. Paul, K. Willecke, and O. Traub. 1993. Gap junction protein connexin40 is preferentially expressed in vascular endothelial and conductive bundles of rat myocardium and is increased under hypertensive conditions. *Circ. Res.* 73:1138–1149.

Bennett, M. V. L., and V. K. Verselis. 1992. Biophysics of gap junctions. *Semin. Cell Biol.* 3:29–47.

Beyer, E., K. E. Reed, E. M. Westphal, H. L. Kanter, and D. M. Larson. 1992. Molecular cloning and expression of rat connexin40, a gap junction protein expressed in vascular smooth muscle. *J. Membr. Biol.* 127:69–76.

Bruzzone, R., J.-A. Haefliger, R. L. Gimlich, and D. L. Paul. 1993. Connexin40, a component of gap junctions in vascular endothelium, is restricted in its ability to interact with other connexins. *Mol. Biol. Cell.* 4:7–20.

Bukauskas, F. F., C. Kempf, and R. Weingart. 1992a. Electrical coupling between cells of the insect Aedes albopictus. *J. Physiol.* 448:321–337.

Bukauskas, F. F., C. Kempf, and R. Weingart. 1992b. Cytoplasmic bridges and gap junctions in an insect cell line (*Aedes albopictus*). *Exp. Physiol.* 77:903–911.

Bukauskas, F. F., and R. Weingart. 1993a. Temperature dependence of gap junction properties in neonatal rat heart cells. *Pflügers Arch.* 423: 133–139.

Bukauskas, F. F., and R. Weingart. 1993b. Multiple conductance states of newly formed single gap junction channels between insect cells. *Pflügers Arch.* 423:152–154.

Bukauskas, F. F., and R. Weingart. 1994. Voltage-dependent gating of single gap junction channels in an insect cell line. *Biophys. J.* 67:1–13.

Chanson, M., K. J. Chandross, M. B. Rook, J. A. Kessler, and D. C. Spray. 1993. Gating characteristics of a steeply voltage-dependent gap junction channel in rat Schwann cells. *J. Gen. Physiol.* 102:925–946.

Chen, Y.-H., and R. L. DeHaan. 1992. Multiple channel conductance states and voltage regulation of embryonic chick cardiac gap junctions. *J. Membr. Biol.* 127:95–111.

Churchill, D., S. Coodin, R. R. Shivers, and S. Caveney. 1993. Rapid de novo formation of gap junctions between insect hemocytes in vitro: a freeze-fracture, day-transfer and patch-clamp study. *J. Cell Sci.* 104: 763–772.

De Mazière, A., L. Analbers, H. J. Jongsma, and D. Gros. 1993. Immunoelectron-microscopic visualization of the gap junction protein connexin40 in the mammalian heart. *Eur. J. Morphol.* 31:51–54.

DeVries, S. H., and E. A. Schwartz. 1992. Hemi-gap junction channels in solitary horizontal cells of the catfish retina. *J. Physiol.* 445:201–230.

Ebihara, L. 1993. Expression of dog connexin 40 in paired Xenopus oocytes. *In* Proceedings of the International Meeting on Gap Junctions, Hiroshima. Y. Kanno, editor. 20.

Eckert, R. 1993. Biophysikalische Charakterisierung von Gap-junction-Kanälen in Säugerzellkulturen. Ph.D. thesis. Universität Stuttgart, Deutschland.

Eckert, R., A. Dunina-Barkovskaya, and D. F. Hülser. 1993. Biophysical characterization of gap-junction channels in HeLa cells. *Pflügers Arch.* 424:335–342.

Elfgang, C., R. Eckert, H. Lichtenberg-Fraté, A. Butterweck, O. Traub, R. A. Klein, D. Hülser, and K. Willecke. 1995. Specific permeability and selective formation of gap junction channels in connexin-transfected HeLa cells. *J. Cell Biol.* In press.

Gourdie, R. G., N. J. Severs, C. R. Green, S. Rothery, P. Germroth, and R. P. Thompson. 1993. The spatial distribution and relative abundance of gap-junctional connexin40 and connexin43 correlate to functional properties of components of the cardiac atrioventricular conduction system. *J. Cell Sci.* 105:985–991.

Gros, D., T. Jarry-Guichard, I. Ten Velde, A. de Mazière, M. J. A. van Kempen, J. Davoust, J. P. Briand, A. F. M. Moorman, and H. J. Jongsma. 1994. Restricted distribution of connexin40, a gap junctional protein, in mammalian heart. *Circ. Res.* 74:839–851.

Haefliger, J.-A., R. Bruzzone, N. A. Jenkins, D. J. Gilbert, N. G. Copeland, and D. L. Paul. 1992. Four novel members of the connexin family of gap junction proteins. *J. Biol. Chem.* 267:2057–2064.

Hennemann, H., T. Suchyna, H. Lichtenberg-Fraté, S. Jungbluth, E. Dahl, J. Schwarz, B. J. Nicholson, and K. Willecke. 1992. Molecular cloning and functional expression of mouse connexin40, a second gap junction gene preferentially expressed in lung. *J. Cell Biol.* 117:1299–1310.

Kanter, H. L., J. E. Saffitz, and E. C. Beyer. 1992. Cardiac myocytes express multiple gap junction proteins. *Circ. Res.* 70:438–444.

Moreno A. P., M. B. Rook, G. I. Fishman, and D. C. Spray. 1994. Gap junction channels: distinct voltage-sensitive and -insensitive conductance states. *Biophys. J.* 67:113–119.

Musil L. S., B. C. Cunningham, G. M. Edelman, and D. A. Goodenough 1990. Differential phosphorylation of the gap junction protein connexin43 in junctional communication-competent and -deficient cell lines. *J. Cell Biol.* 111:2077–2088.

Robinson, R. A., and R. H. Stokes. 1970. Electrolyte Solutions. Butterworths, London. 465 pp.

Suchyna, T. M., L. X. Xu, F. Gao, C. R. Fourtner, and B. J. Nicholson. 1993. Identification of proline residue as a transduction element involved in voltage gating of gap junctions. *Nature.* 365:847–849.

Traub, O., R. Eckert, H. Lichtenberg-Fraté, C. Elfgang, B. Bastide, K. H. Scheidtmann, D. F. Hülser, and K. Willecke. 1994. Immunohistochemical and electrophysiological characterization of murine connexin40 and -43 in mouse tissues and transfected human cells. *Eur. J. Cell Biol.* 64: 101–112.

Veenstra, R. D., H.-Z. Wang, E. C. Beyer, S. V. Ramanan, and P. R. Brink. 1994. Connexin37 forms high conductance gap junction channels with subconductance state activity and selective dye and ionic permeabilities. *Biophys. J.* 66:1915–1928.

Weingart, R. 1986. Electrical properties of the nexal membrane studied in rat ventricular cell pairs. *J. Physiol.* 370:267–284.

Weingart, R. 1993. Gating properties of cardiac gap junctions. *In* Proceedings of the 32nd Congress of the International Union of Physiological Sciences, Glasgow. 337.

Weingart, R., and F. F. Bukauskas. 1993. Gap junction channels of insect cells exhibit a residual conductance. *Pflügers Arch.* 424:192–194.